



HAL
open science

Theoretical demonstration of a hot-carrier effect in ultra-thin solar-cell

Nicolas Cavassilas, Imam Makhfudz, Anne-Marie Daré, Michel Lannoo, Guillaume Dangoisse, Marc Bescond, Fabienne Michelini

► **To cite this version:**

Nicolas Cavassilas, Imam Makhfudz, Anne-Marie Daré, Michel Lannoo, Guillaume Dangoisse, et al.. Theoretical demonstration of a hot-carrier effect in ultra-thin solar-cell. *Physical Review Applied*, 2022, 17 (6), pp.064001. 10.1103/PhysRevApplied.17.064001 . hal-03833978

HAL Id: hal-03833978

<https://hal.science/hal-03833978v1>

Submitted on 28 Oct 2022

HAL is a multi-disciplinary open access archive for the deposit and dissemination of scientific research documents, whether they are published or not. The documents may come from teaching and research institutions in France or abroad, or from public or private research centers.

L'archive ouverte pluridisciplinaire **HAL**, est destinée au dépôt et à la diffusion de documents scientifiques de niveau recherche, publiés ou non, émanant des établissements d'enseignement et de recherche français ou étrangers, des laboratoires publics ou privés.

Theoretical demonstration of a hot-carrier effect in ultra-thin solar-cell

Nicolas Cavassilas¹, Imam Makhfudz¹, Anne-Marie Daré¹, Michel Lannoo¹, Guillaume Dangoisse^{2,3}, Marc Bescond^{1,2} and Fabienne Michelini¹

¹*Aix Marseille Université, CNRS, Université de Toulon, IM2NP UMR 7334, 13397, Marseille, France*

²*LIMMS-CNRS, IRL 2820, 4-6-1 Komaba, Meguro-ku, Tokyo 153-8505, Japan*

³*Ecole Normale Supérieure de Paris, Université PSL, Sorbonne Université, Université de Paris, 75005 Paris, France, 24 rue Lhomond F75005 Paris, France*

Based on a quantum modeling of the electronic transport, this work shows that ultra-thin solar cells can exhibit an improved open-circuit voltage V_{oc} , without current reduction. This improvement is obtained when an energy-selective contact is considered between the absorber and the reservoir, and is attributed to a hot-carrier effect. While extraction with a non-selective contact does not generate hot-carriers, the use of energy-selective contact induces an increase of carrier temperature up to 130 K and a corresponding V_{oc} enhancement of 41 meV, considering an InGaAs absorber. This enhancement agrees with a simple and general expression formulated in the quantum thermal machine field. Concerning the current, we show that current through an energy-selective contact is of the same order of magnitude as the one obtained without selectivity. This remarkable behavior, which is explained by the hybridation of states in the absorber with the state of the contact, requires a quantum confinement and thus an ultra-thin absorber.

I INTRODUCTION

The hot-carrier solar cell (HCSC) is an elegant concept¹ allowing, in theory, to exceed the limit of Shockley-Queisser (SQ)². The idea, as shown in Fig. 1, is that the carriers remain hot in the absorber where they have been photo-generated by a hot source (the sun). Extracting these carriers through energy-selective contacts (for instance at given energies E_n and E_p for electrons and holes respectively) we can theoretically recover this excess of thermal energy in the form of voltage in the reservoirs. The open-circuit voltage can be formally obtained by a simple expression by assuming two different local thermal equilibria for the reservoirs and the absorber, and sharp energy filters between these equilibria. To do so, we consider the entropy balance³ of the transfer of an electron at energy E_n from the absorber (with a Fermi level μ_{na} and a temperature T_a) to the n-reservoir (with a Fermi level μ_n and at lattice temperature T_L)

$$\Delta S = -\frac{E_n - \mu_{na}}{T_a} + \frac{E_n - \mu_n}{T_L}. \quad (1)$$

The perfect energy selectivity enables an isentropic transfer with $\Delta S = 0$. In this case Eq.(1) shows that both electronic distributions in the absorber and in the n-reservoir must have the same value at the transfer energy E_n .³ Doing the same analysis for holes at the transfer energy E_p , and summing the two expressions, we finally get^{1,4}

$$V_{oc} = \left(1 - \frac{T_L}{T_a}\right) E_{ext} + \Delta\mu_a \frac{T_L}{T_a} \quad (2)$$

with $V_{oc} = \mu_n - \mu_p$, the open-circuit voltage, $E_{ext} = E_n - E_p$ and $\Delta\mu_a = \mu_{na} - \mu_{pa}$. This expression was derived in the context of quantum thermal machine³ and extrapolated to the solar cell field^{1,4-6}. This equation shows that if $T_a = T_L$ (no hot-carriers), we obtain $V_{oc} = \Delta\mu_a = \Delta\mu_L$, i.e. the Fermi level splitting when the carriers in the absorber are at the lattice temperature. In this case, which corresponds to a conventional solar cell, V_{oc} is directly related to the rate of the radiative generation and recombination in the absorber and therefore, to its energy bandgap E_g , leading to the SQ limit. On the other hand, if $T_a \gg T_L$ and if electrons and holes are close to equilibrium (for example due to impact ionization)⁷, we then have $\Delta\mu_a \approx 0$ and consequently $V_{oc} \approx E_{ext}$. It is then possible to consider a material for the absorber with a small E_g , to have a significant short circuit current, while considering a contact offering a large E_{ext} , to have a large V_{oc} . We are therefore freed from the trade-off on E_g at the origin of the SQ limit.

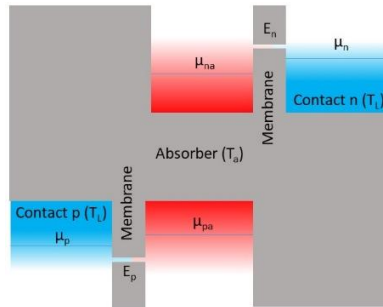


Figure 1. Schematic representation of a hot-carrier solar cell. In the absorber the electron- and hole-distributions are defined by the Fermi levels μ_{na} and μ_{pa} and by the temperature T_a . In both reservoirs the temperature is given by the lattice temperature T_L . The electron-distribution in n-reservoir is defined by μ_n while the hole-distribution in p-reservoir is defined by μ_p . Carriers can transit from the absorber into the reservoirs through contacts at energies E_n and E_p , for electrons and holes, respectively.

In practice, the main difficulty in the development of such solar cells is to obtain a hot-carrier effect, generating a V_{oc} improvement, without degrading the extraction of carriers to preserve the current. Indeed, in isolated system (without contact), hot-carrier distributions have been observed under light illumination in steady-states.⁸⁻¹⁰ In such systems the carriers are generated at an average energy $E_{gen} = k_B T_{gen}$ strongly larger than $k_B T_L$. The carriers cool down in a two-step process: *i)* they lose energy by optical-phonon emission, and *ii)* each optical-phonon splits into two acoustic phonons. Assuming a reservoir of acoustic-phonons at the lattice temperature T_L , generated carriers thermalize at an energy T_c located between T_{gen} and T_L . If the cooling rate is larger than the generation rate, T_c is close to T_L , while if the generation rate is larger than the cooling rate, T_c is close to T_{gen} .¹¹ The goal is thus to increase the generation rate with a large power illumination, and to reduce the cooling rate. In case where the cooling is limited by the optical-acoustic rate, hot-carriers emit optical phonons which are preferentially reabsorbed by the carriers rather than split into two acoustic phonons. This behavior seems to be at the origin of hot-carrier in bulk^{10,11} but could also explain observations made in quantum wells.¹² Moreover, in quantum well, due to more restrictive selection rules, the carrier-optical phonon rate can also be reduced. In all cases, these strategies to reduce the cooling rate are called the phonon bottleneck.

In opposition to an isolated system, we can consider a system in which the absorber is perfectly connected to a reservoir. This means that electronic states of the absorber are totally delocalized in the reservoir and vice versa. A priori, the most favorable case is when a generated hot-carrier can ballistically reach the reservoir, before experiencing an optical phonon emission. However, once in the reservoir, such an electron cools down. Moreover, at V_{oc} , the ballistic carrier is replaced by a cold carrier coming from the reservoir. Hence, the electronic distribution in the absorber is almost equal to that of the reservoir and hot-carrier effect cannot be observed.

A practical HCSC has to maintain the carriers hot by isolating the absorber from the cold reservoir, and on the other hand, it has to enable an efficient extraction of carriers. Those two requirements might be seen as contradictory, but quantum mechanism can break this paradox. As we have already shown,¹³ if the absorber is a quantum well, one of the confined states hybridizes with the resonant state in the energy-selective contact. It results an efficient extraction of the photo-generated carriers than can be assisted by phonon scattering. This hybridation is equivalent to delocalize the absorber states into the reservoir, but only at a chosen energy-window. For the other energies, and particularly when the electronic distribution in the reservoir is larger than that in the absorber (close to the band edge), the isolation has to be severely preserved.

In this theoretical article, we confirm that the use of an ultra-thin absorber enables to implement the hot electron strategy. In such a structure, considering an electron selective contact, consisting of a double barrier and a quantum dot (QD) or a quantum well (QW), our numerical calculations show that V_{oc} varies with the extraction energy E_n . Since such variations of V_{oc} are consistent with equation (2), they are attributed to the hot-carrier behavior. Moreover, we confirm that the absorption current is preserved by the energy-selective contact. Advances in the fabrication of ultra-thin solar cells, based both on the control of contacts and on the photonic environment, could therefore result in HCSC development.¹⁴

II. METHODOLOGY

To carry out this study, we model ultra-thin cells with the non-equilibrium Green's functions (NEGF) formalism in a self-consistent framework with the Poisson equation. This physical model, which includes the effects of interactions in a picture of quantum transport, is widely used in the field of semiconductor quantum devices.¹⁵⁻¹⁷ It indeed enables to accurately consider behaviors such as quantum confinement, tunneling, electron-phonon and electron-photon scatterings and to model the effects of the semi-infinite reservoirs.

Here, we consider a multi-unidimensional model,¹⁵ meaning that we consider a unidimensional potential along the transport direction, and an invariant potential in transverse plane. In this plane, the dispersions of electron and hole are reproduced by a discretization of the transverse wave-vector k_{\perp} . For these dispersions we assume the effective mass approximation, excepted in QD, where no dispersion is considered. This approximation is also assumed in the transport direction. At the boundaries of the devices, in the transport direction, we assume semi-infinite reservoirs meaning that the potential in the reservoir is invariant on semi-infinite length.

Concerning scatterings, for this study, we consider electron-photon, electron-optical phonon and electron-acoustic phonon scatterings. For scattering with photons, in order to assume conditions close to the experimental ones,¹⁸ we consider that the cells are illuminated by a 954 nm laser with a power of 1 kW.cm⁻². On the other hand, the cells can emit photons at any energy, such an emission being due to the interband radiative recombination. Note that we assume the radiative approximation, i.e. non-radiative recombinations are neglected.

For scattering with phonons, we consider that both optical and acoustic phonons remain at $T_L = 300$ K. Indeed, we only calculate the Green functions of the electrons while phonons are considered at thermodynamical equilibrium. We are aware that this approximation is a limitation of our model. But, this limitation reduces the observed hot-carrier effect. Thus, our model cannot overestimate the conclusions of the present work.

Another substantial approximation is that we do not consider the electron-electron interaction in the active region. This scattering does not diffuse energy and therefore does not participate to the cooling. But it favors the transition from an out-of-equilibrium distribution to a Fermi distribution. This approximation explains why the distribution obtained in the present work are not well described by a Fermi function. Note that this interaction is intrinsically taken into account in the reservoir in which Fermi distributions at room temperature are imposed.

Finally, our model allows us to calculate the electronic density and the electronic density-of-states, both versus position and energy. This enables us to extract the corresponding electronic distribution. We can also calculate the absorption and recombination currents as functions of the voltage applied between the two reservoirs, allowing to obtain V_{oc} .

III. RESULTS

Figure 2 represents the band diagrams and the current spectra obtained for three different contacts at a voltage of 0.7 V ($\mu_p = 0$ eV and $\mu_n = 0.7$ eV). This contact is either a simple tunnel barrier (Fig. 2a), thus non-selective, or a QD between two tunnel barriers (Fig. 2b and c), thus selective. In Figs. 2b and c the size of the QD varies, thus modifying the extraction energy E_n (0.94 eV and 1.02 eV respectively). In all three

cases, we consider an InGaAs absorber, 12 nm thick, with an InP p-reservoir and an InGaP wetting layer. The n-reservoir is also made of InP but is separated from the absorber by the contact.

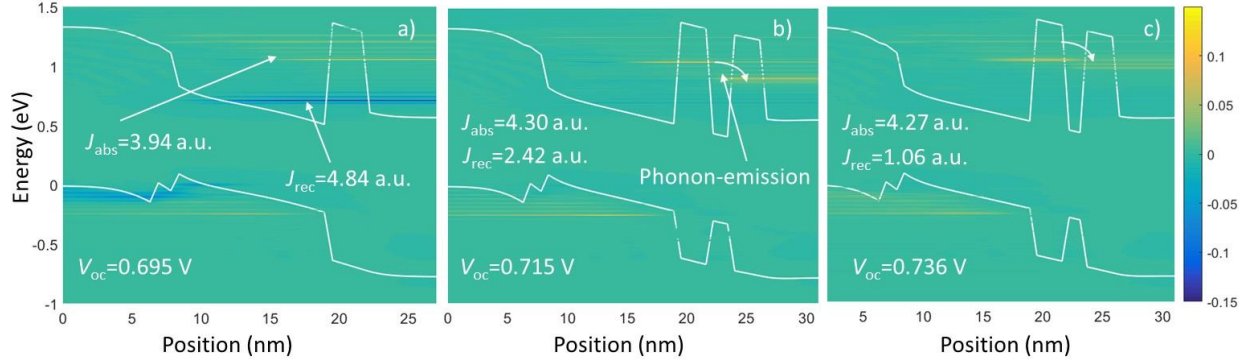


Figure 2. Band diagrams and mapping of the current spectra of the ultrathin InGaAs solar cell (12 nm), a) with a non-selective contact, b) with a selective contact with $E_n=0.94$ eV and, c) with $E_n=1.02$ eV. In all cases the reservoirs are in InP and contacts between the absorber and the n-reservoir are made with barrier of AlGaAsSb. For the selective contact, we assume a QD between the two barriers. The Fermi level in p-reservoir is $\mu_p=0$ eV, while in n-reservoir $\mu_n=0.7$ eV.

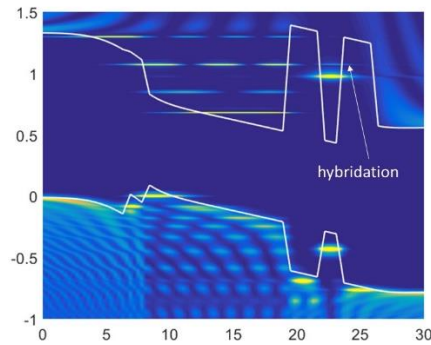


Figure 3. Band diagram and mapping of the local density of states of one transverse mode k_t calculated in the device presented Fig. 2c with $E_n=1.02$ eV. Between the two barriers, in the QD, the local density of states shows 2 states. The higher one is due to the hybridation with the third state in the absorber. The consequence of this hybridation is that electrons on this third state is delocalized in the reservoir.

As shown in Fig. 2, the absorption currents¹⁹ J_{abs} are 3.94, 4.3 and 4.27 in arbitrary unit, for the cell without selectivity and for $E_n=0.94$ eV and 1.02 eV, respectively. In the three cells, the electronic densities of states in the absorber are similar. The difference in the absorption currents is thus not attributed to absorption but rather to extraction which is thus pretty more efficient when the contact is selective. To explain this result, we represent in Fig. 3 the density-of-states in the cell with $E_n=1.02$ eV. The third state of the absorber hybridizes with the state in the QD.¹³ An electron on this state is thus delocalized in the contact and then in the reservoir. Moreover, thanks to the assistance of optical phonon-emission, this extraction is even more efficient. This phonon-assisted extraction can be seen on the current-spectra represented in Fig. 2, where in case of non-selective contact the current absorption (the positive one) is ballistic, while phonons contribute in the cases of selective contacts. Such a hybridization appears only when electrons are confined in absorber. In case of a bulk absorber, as considered theoretically²⁰ and experimentally,²¹ a consequent reduction in current is observed with selective contact. Concerning the recombination current (the negative contribution on current spectra in

Fig. 2), at a given bias, the amplitude is reduced with the selective contacts. This confirms that the isolation, at band-edge, is much more efficient with the double-barrier.

Concerning the open-circuit voltage, V_{oc_num} , we obtain 0.695 V (non-selective), 0.715 V ($E_n = 0.94$ eV) and 0.736 V ($E_n = 1.02$ eV). We see that the non-selective contact cell offers the weakest V_{oc_num} and that V_{oc_num} increases with the extraction energy E_n . We then calculate the electronic distribution in the absorber and in the n-reservoir. These distributions are plotted as a function of the energy on Fig. 4 for the three devices of Fig. 2. As expected, the distribution in the three n-reservoirs is exactly equal to the Fermi function with $\mu_n=0.7$ eV and $T=300$ K. When considering a simple tunnel barrier (Fig. 4a), the distribution in the absorber is almost equal to this distribution, i.e. no hot-carrier effect is observed. With a selective contact (Fig. 4b and c), the distributions in the absorber are unusual and correspond to out-of-equilibrium electrons. We first see that they depict peaks. Observation of the distribution for each transverse wave-vector k_t shows that these peaks are related to the optical phonon, since they are spaced apart by the energy of the optical phonon. Independently of these peaks, we propose to fit (insets of Fig. 4) these two distributions by a Fermi function. We obtain $\mu_{na}=0.62$ eV and $T_a=430$ K for $E_n=0.94$ eV and $\mu_{na}=0.6$ eV and $T_a=430$ K for $E_n=1.02$ eV. Even though we cannot rigorously consider an equilibrium and thus a temperature, this result shows that such selective contacts isolate well enough the absorber, from the reservoirs, to allow the electrons in the absorber to maintain a hot pseudo-equilibrium. This result also shows that a hot equilibrium can be obtained although optical phonons are at lattice temperature. Considering hot phonons should increase the electronic temperature.

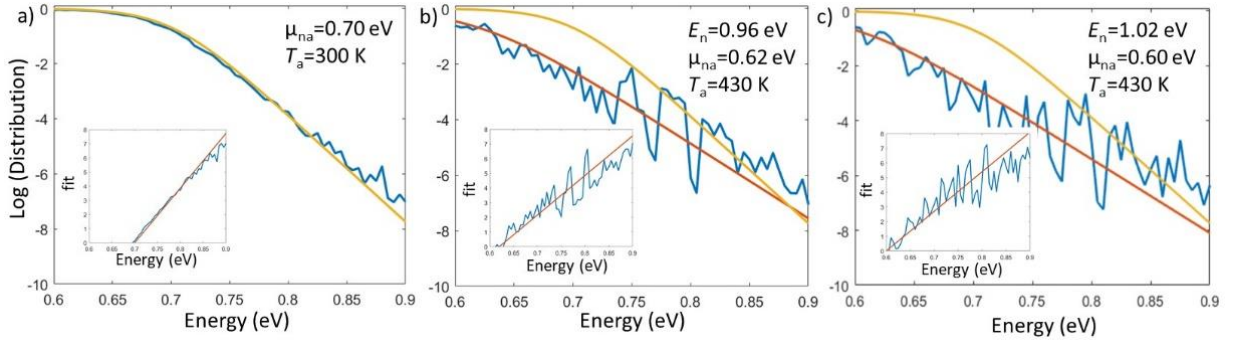


Figure 4. Natural logarithm of the electronic distribution, versus energy, of cells presented in Fig. 2, in absorber (blue line) and in n-reservoir (yellow line). We also represent, in red, the fit of the distribution in the absorber obtained with a Fermi function. To obtain easily this fit we represent $\text{fit}=\log(1/\text{distribution}-1)$ versus the energy. The corresponding curves are in inset.

To confirm the link between V_{oc} and this hot pseudo-equilibrium distribution, we modify equation (2) in order to consider the holes are at T_L . Indeed, as expected (very strong hole-optical phonon scattering and no contact for the p-reservoir) there is no hot holes. We then obtain this new equation for V_{oc_an} (an for analytical):

$$V_{oc_an} = \left(1 - \frac{T_L}{T_a}\right) E_n + \mu_{na} \frac{T_L}{T_a} - \mu_p. \quad (3)$$

By applying this expression to the two cells with $E_n=0.94$ eV and 1.02 eV, and by considering the corresponding μ_{na} and T_a , we find respectively $V_{oc_an}=0.717$ V and 0.727 V (versus $V_{oc_num} = 0.715$ V and 0.736 V obtained by simulations). These values should be compared to 0.695 V, the numerical V_{oc} obtained without hot-carriers. The agreement between the numerical and the analytical values confirms that the improvement of V_{oc_num} with the selectivity of contact is due to a hot-carriers effect.

We also conducted calculations for a semi-selective contact considering a quantum well (QW) rather than a QD. In this case, with $E_n=1.02$ eV, we obtain numerically $V_{oc_num}=0.728$ V, $\mu_{na}=0.62$ eV and $T_a=400$ K, which gives $V_{oc_an}=0.720$ V. Even in the case with QW, the numerical and analytical values are in good agreement. Compared to the case with the QD contact having the same E_n , all the criteria show that the carriers are less hot. A selective contact is necessary for optimal operation, but, despite the semi-selectivity, the effect of hot-carriers is significant. Since it is much easier to fabricate a semi-selective contact, this result is very encouraging for a future experimental demonstration of HCSC.

IV. DISCUSSION

In this chapter we propose a discussion based on a simple rate-model which is schematically represented Fig. 5. We consider three electronic states numbered 1, 2 and 3 at energies $E_1 < E_2 < E_3$ ($E_n = \hbar\omega(n - 1)$) with $\hbar\omega$ the phonon energy) and with the distributions f_1, f_2 and f_3 . By emission or absorption of phonon, electrons can change of state with the respective rates τ_{em} and τ_{ab} . Supposing $n > m$, the electrons flux between the states n and m is given by $\tau_{em}f_n(1 - f_m) - \tau_{ab}f_m(f_n - 1)$. We also consider a radiative generation flux G , corresponding to the laser excitation, arriving into the top state 3. This involves a recombination flux from each state n given by Rf_n , with $G = R(f_1 + f_2 + f_3)$ at V_{oc} . In stationary regime the net flux on any state equals zero and we can calculate f_1 and f_3 versus f_2 and the other parameters

$$f_1 = \frac{-G \frac{f_1}{f_1+f_2+f_3} + \tau_{em}f_2}{\tau_{ab} + f_2(\tau_{em} - \tau_{ab})} \quad (4)$$

$$f_3 = \frac{G \frac{f_1+f_2}{f_1+f_2+f_3} + \tau_{ab}f_2}{\tau_{em} - f_2(\tau_{em} - \tau_{ab})}. \quad (5)$$

Fig. 5a shows result obtain for $f_2 = 10^{-4}$, with $G = 0$, at the thermodynamical equilibrium. We assume $\tau_{ab} = MN$, and $\tau_{em} = M(1 + N)$ with M the scattering matrix element and N the number of optical phonons which is given by the Bose distribution at 300 K. In this case the resulting distribution f_n , which does not depend on M , exhibits the shape of a Boltzmann distribution at 300 K. This simple rate-model enables thus to describe electrons at the equilibrium with the phonons.

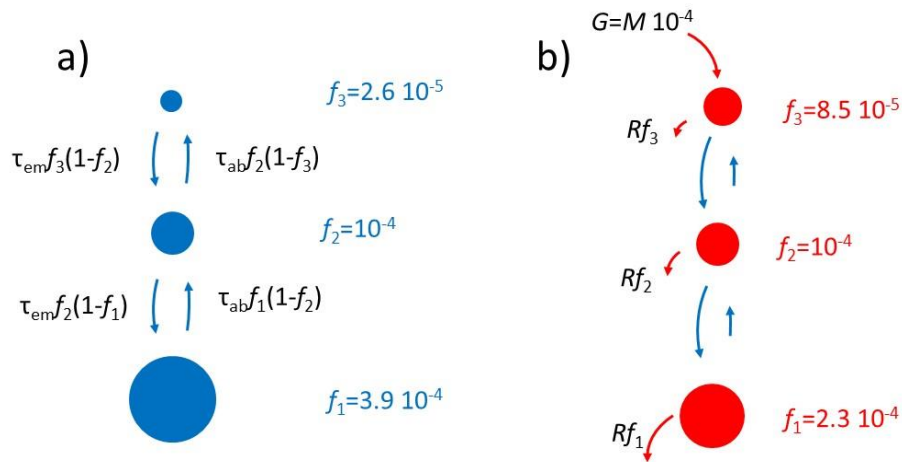


Fig. 5. Schematic representation of the rate-model and of the resulting distribution a) at the thermodynamical equilibrium, and b) with a radiative generation on the top state 3. The surfaces of the disk n are proportional to the corresponding distributions f_n . For both calculations f_2 is imposed to 10^{-4} and the number of phonons is unchanged (phonons stay cool).

We present in Fig. 5b the resulting f_n when $G = M 10^{-4}$. As suggested in the two equations (4) and (5), with a generation G at the top state E_3 , the distribution at high energy increases while it is reduced at low energy E_1 . The electrons are no more at the equilibrium (f_n does not exhibit an exponential shape) but the corresponding average temperature (800 K) is larger than the room temperature and increases with G . We thus obtain a pseudo hot equilibrium simply by generating electrons at higher energy than the average energy of the corresponding recombination. This result is in agreement with the numerical calculation presented in this work and shows that, even with cold phonons, in an isolated absorber it is possible to obtain a pseudo hot equilibrium. For that, G , compared to the scattering rates, has to be large enough.

We now consider that this pseudo hot distribution is an absorber connected to the cold distribution, which is the reservoir. Fig. 6a shows when an isentropic extraction is considered, meaning with a selective contact whose energy E_n is located such that the hot and cold distributions are equal. In this case, at V_{oc} , the hot distribution is not disturbed by the contact. On the other hand, Fig. 6b shows when a non-selective contact is considered. Such a contact reduces the distribution of the absorber at high energy while it increases it at low energy. In other words, such a contact cools down the electrons in the absorber. These results are also in agreement with the numerical calculations conducted in the present work.

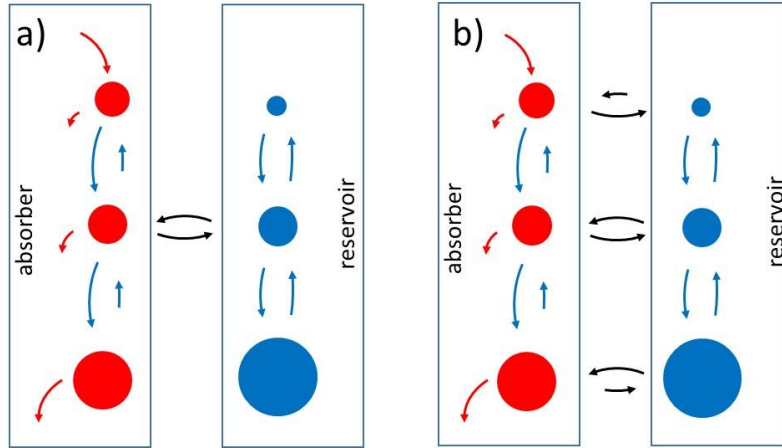


Fig. 6. Schematic representation of a hot absorber connected to a cold reservoir at V_{oc} with a) a selective contact allowing an isentropic extraction, and b) with a non-selective contact. While the isentropic extraction does not modify the electronic distribution in the absorber, the non-selective contact cools down the electrons in the absorber.

IV. CONCLUSION

This article shows that, under powerful laser illumination, an ultra-thin solar cell associated with energy-selective contact exhibits a larger V_{oc} without current degradation. In spite of the selective contact our quantum model shows that the current is not degraded thanks to a hybridization behavior. The improvement of V_{oc} is related to a hot-carrier effect which can be explained by a simple rate model. Such an effect increases with the selectivity but still exists in realistic design such as contact made with QW. This result should be more visible by considering hot phonons and should not be reduced by the carrier-carrier scattering. This behavior could be experimentally demonstrated by the V_{oc} comparison of ultra-thin solar cells with a simple barrier and with a double-barrier as contact. If the current is not degraded by the selectivity, as shown by our results, such a measurement would be a demonstration of a hot-carrier solar cell operation.

Moreover, an interesting result shown in this article is that, assuming a sophisticated numerical model including realistic materials under illumination, we confirm the validity of the very general expression of V_{oc} (eq. (2)), in both QD and QW geometries.

In the future, a study concerning the design of the contact would be interesting to better understand the impact of hybridation and selectivity in cell under a concentrated solar spectrum.

ACKNOWLEDGEMENT

The authors thank ICEMAN (ANR-19-CE05-000) for financial support.

DATA AVAILABILITY STATEMENT

The data that support the findings of this study are available from the corresponding author upon reasonable request.

CONFLICT OF INTEREST

The authors have no conflicts to disclose.

REFERENCES

- ¹R. T. Ross and A. J. Nozik, "Efficiency of hot-carrier solar energy converters," *J. Appl. Phys.* **53**(5), 3813–3818 (1982).
- ²W. Shockley and H. J. Queisser, "Detailed balance limit of efficiency of p-n junction solar cells," *J. Appl. Phys.* **32**(3), 510–519 (1961).
- ³T. E. Humphrey, R. Newbury, R. P. Taylor, and H. Linke, "Reversible Quantum Brownian Heat Engines for Electrons," *Phys. Rev. Lett.* **89**(11), 116801-116805 (2002).
- ⁴A. Pusch, M. Dubajic, M. P. Nielsen, G. J. Conibeer, S. P. Bremner, and N. J. Ekins-Daukes, "Optoelectronic reciprocity in hot carrier solar cells with ideal energy selective contacts," *Prog. Photovolt. Res. Appl.* **29**, 433-444 (2021).
- ⁵S. C. Limpert and S. P. Bremmer, "Hot carrier extraction using energy selective contacts and its impact on the limiting efficiency of a hot carrier solar cell", *App. Phys. Lett.* **107**, 073902 (2015).
- ⁶S. C. Limpert, S. Bremmer and H. Linke, "Reversible electron-hole separation in a hot carrier solar cell", *New J. Phys.* **17**, 095004 (2015).
- ⁷P. Würfel, "Solar energy conversion with hot impact ionization," *Solar Energy Materials and Solar Cells* **46**, 43-52 (1997).
- ⁸D.-T. Nguyen, L. Lombez, F. Gibelli, S. Boyer-Richard, A. Le Corre, O. Durand, J.-F. Guillemoles, "Quantitative experimental assessment of hot carrier-enhanced solar cells at room temperature," *Nature Energy* **3**(3), 236-242 (2018).
- ⁹L.C. Hirst, H. Fujii, Y. Wang, M. Sugiyama, N.J. Ekins-Daukes, "Hot carriers in quantum wells for photovoltaic efficiency enhancement," *IEEE Journal of Photovoltaics* **4**(1), 244-252 (2013).

- ¹⁰M. Giteau, E. de Moustier, D. Suchet, H. Esmailpour, H. Sodabanlu, K. Watanabe, S. Collin, J.-F. Guillemoles, Y. Okad, "Identification of surface and volume hot-carrier thermalization mechanisms in ultrathin GaAs layers," *Journal of Applied Physics* **128**(19), 193102 (2020).
- ¹¹C.-Y. Tsai, "Theoretical model and simulation of carrier heating with effects of nonequilibrium hot phonons in semiconductor photovoltaic devices," *Prog. Photovoltaics Res. Appl.* **26**(10), 808–824 (2018).
- ¹²Y. Zhang, L. Tang, B. Zhang, P. Wang, and C. Xu, "Quantitative study on the mechanisms underlying the phonon bottleneck effect in InN/InGaN multiple quantum wells," *Appl. Phys. Lett.* **116**(10), 103104 (2020).
- ¹³N. Cavassilas, F. Michelini, M. Bescond, T. Joie, "Hot-carrier solar cell NEGF-based simulations," *Physics, Simulation, and Photonic Engineering of Photovoltaic Devices V*, 97430R (2016).
- ¹⁴I. Massiot, A. Cattoni, and S. Collin, "Progress and prospects for ultrathin solar cells," *Nat. Energy* **5**, 959-972 (2020).
- ¹⁵N. Cavassilas, F. Michelini, M. Bescond, "Modeling of nanoscale solar cells: The Green's function formalism," *J. of Renewable and Sustainable Energy* **6**(1), 011203 (2014).
- ¹⁶A. Yangui, M. Bescond, T. Yan, N. Nagai, K. Hirakawa, "Evaporative electron cooling in asymmetric double barrier semiconductor heterostructures," *Nature communications* **10**(1), 1-7 (2019).
- ¹⁷J. Fast, U. Aeberhard, S. Bremner, H. Linke, "Hot-carrier optoelectronic devices based on semiconductor nanowires," *Applied Physics Reviews* **8**(2), 021309 (2021).
- ¹⁸H. Esmailpour, L. Lombez, M. Giteau, A. Delamarre, D. Ory, A. Cattoni, S. Collin, J.-F. Guillemoles, D. Suchet, "Investigation of the spatial distribution of hot carriers in quantum-well structures via hyperspectral luminescence imaging," *J. Appl. Phys.* **128**(16), 165704 (2020).
- ¹⁹B. Galvani, D. Suchet, A. Delamarre, M. Bescond, F. Velia Michelini, M. Lannoo, J.-F. Guillemoles, N. Cavassilas, "Impact of Electron–Phonon Scattering on Optical Properties of CH₃NH₃PbI₃ Hybrid Perovskite Material," *ACS omega* **4** (25), 21487-21493 (2019).
- ²⁰A. P. Kirk and M. V. Fischetti, "Fundamental limitations of hot-carrier solar cells," *Phys. Rev. B* **86**(16), 165206 (2012).
- ²¹S. Limpert, A. Burke, I.-J. Chen, N. Anttu, S. Lehmann, S. Fahlvik, S. Bremner, G. Conibeer, C. Thelander, M.-E. Pistol, "Single-nanowire, low-bandgap hot carrier solar cells with tunable open-circuit voltage," *Nanotechnology* **28**(43), 434001 (2017).